Single molecule evaluation of fluorescent protein photoactivation efficiency using an *in vivo* nanotemplate

Nela Durisic, Lara Laparra-Cuervo, Ángel Sandoval-Álvarez, Joseph S. Borbely, Melike Lakadamyali

Supplementary Information:

Supplementary Figure 1: Evolution of the Glycine receptor expression density on the oocyte membrane

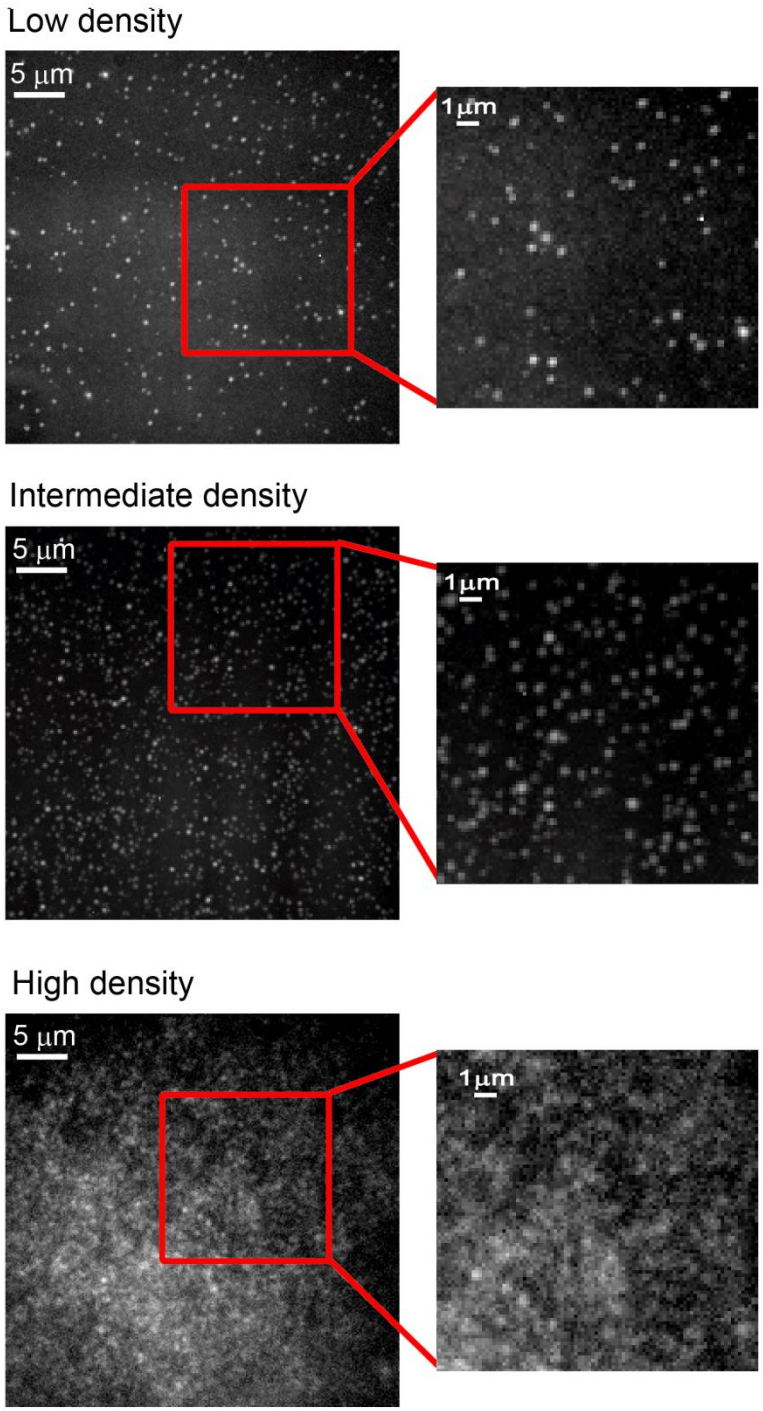

Oocytes imaged at ~12-20 hours after RNA injection showed a low density of GlyR s on their membrane (upper), therefore we could reliably identify and analyze isolated single channels. The expression level slowly evolved towards intermediate (middle) and high (lower) densities at ~4 hours and ~16 hours after the initial expression was observed, providing a large time window in which GlyRs could be imaged at a single channel density.

Supplementary Figure 2: Single step photobleaching with mEos2

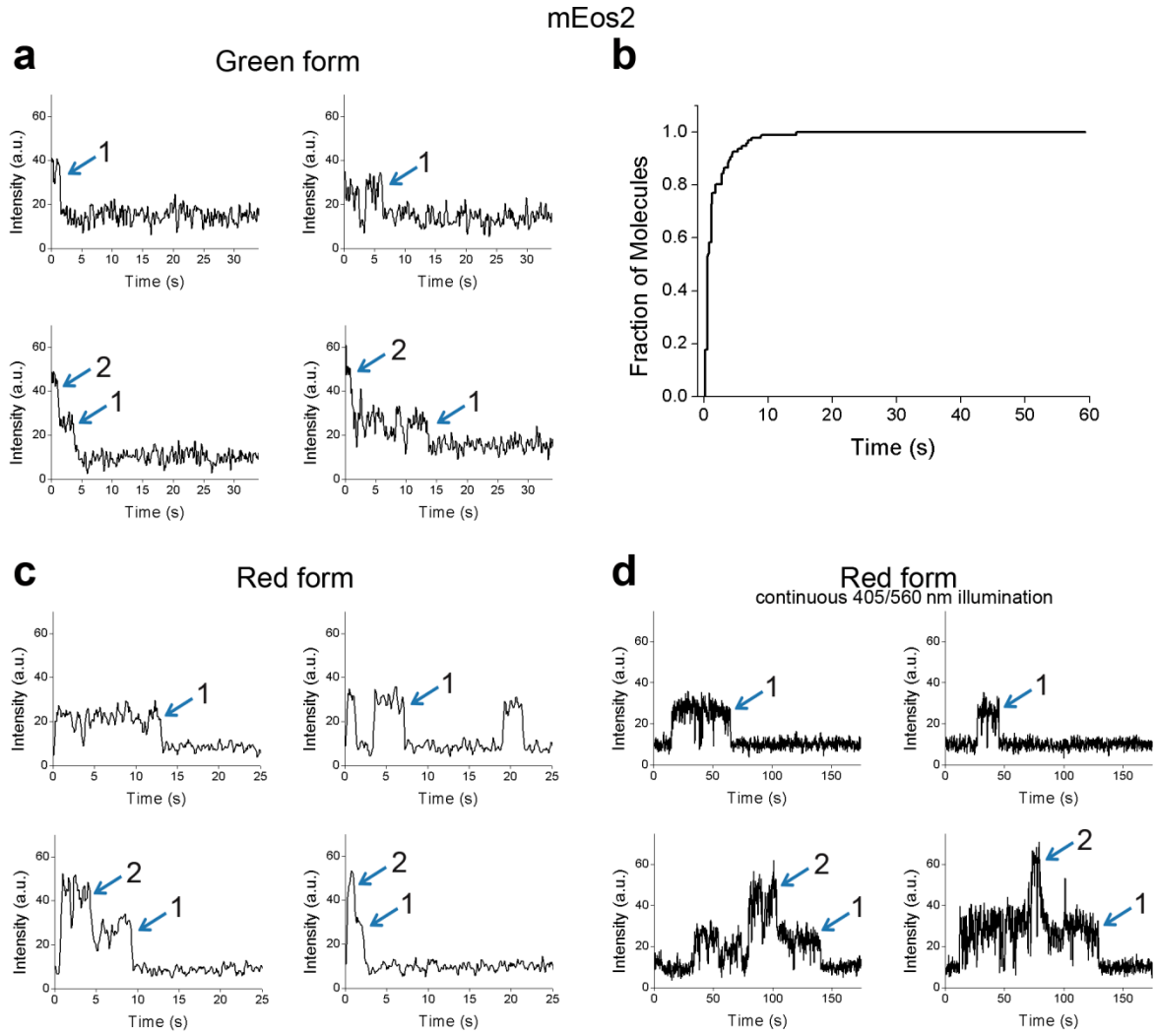

(a) Example intensity-time traces that show single (upper) and double (lower) steps obtained from the native (green) form of mEos2. (b) Cumulative number of photoconverted mEos2 labeled GlyRs showing the photoconversion kinetics for this fluorescent protein under continuous illumination with 6.8 W/cm^2 405 nm laser. The cumulative number has been normalized by the maximum number of detected molecules. (c) Example intensity-time traces that show single (upper) and double (lower) steps obtained from the red form of mEos2 by first illuminating with 405 nm laser to achieve photoconversion and then with 560 nm laser to image and photobleach the photoconverted molecules. (d) Example intensity-time traces that show single (upper) and double (lower) steps obtained from the red form of mEos2 by simultaneous and continuous illumination with 405 nm and 560 nm laser. The rising steps in the beginning of the intensity-time traces are due to the individual photoconversion events and the falling steps at the end of the intensity-time traces are due to the individual photobleaching events. All traces have been averaged using a rolling average of adjacent two points in the trace to smooth noise.

Supplementary Figure 3: Single step photobleaching with Dendra2

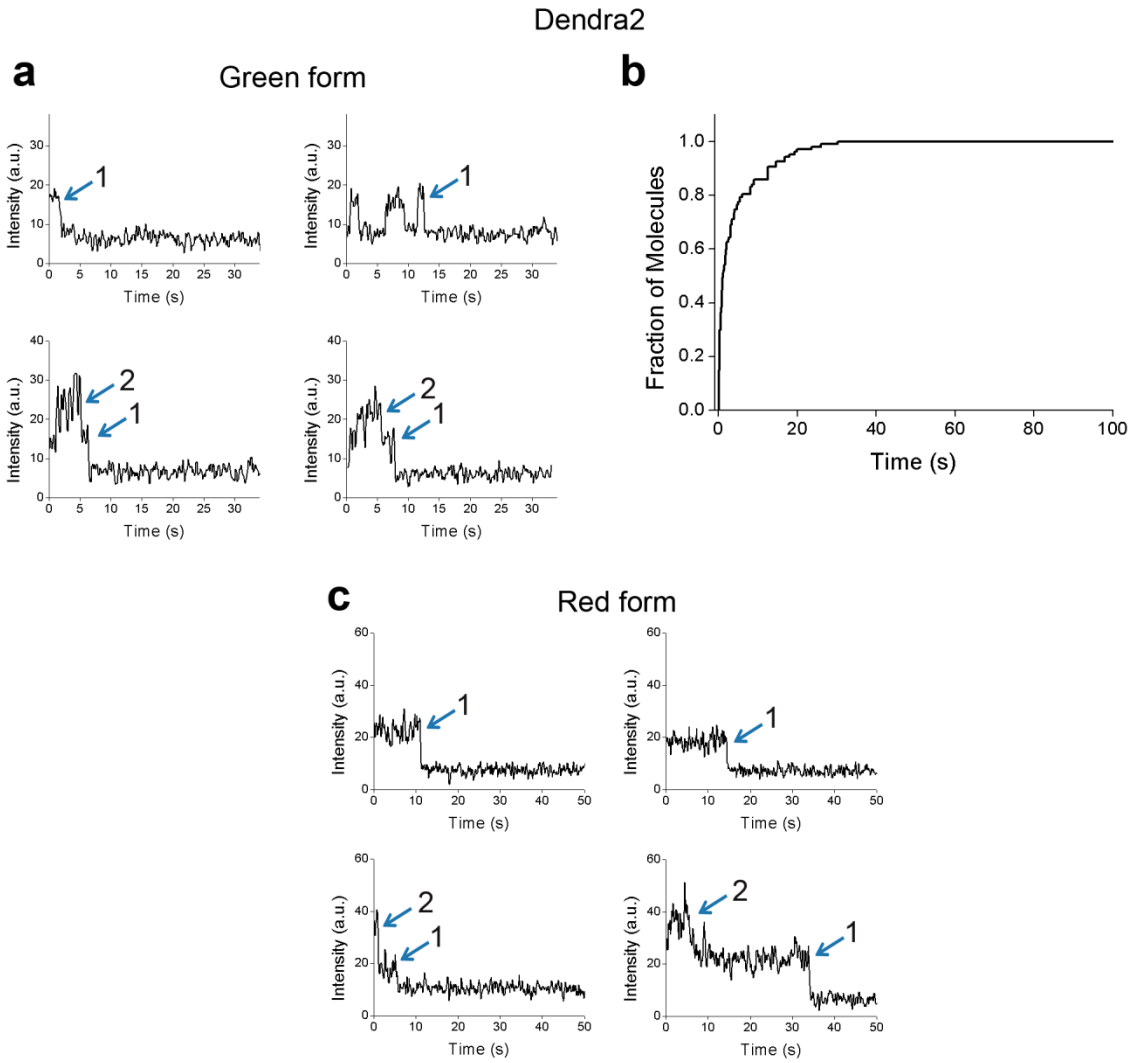

(a) Example intensity-time traces that show single (upper) and double (lower) steps obtained from the native (green) form of Dendra2. (b) Cumulative number of photoconverted Dendra2 labeled GlyRs showing the photoconversion kinetics for this fluorescent protein under continuous illumination with 1.5 W/cm^2 405 nm laser. The cumulative number has been normalized by the maximum number of detected molecules. (c) Example intensity-time traces that show single (upper) and double (lower) steps obtained from the red form of Dendra2 after photoconversion with 405 nm laser illumination. All traces have been averaged using a rolling average of adjacent two points in the trace to smooth noise.

Supplementary Figure 4: Single step photobleaching with mClavGR2 and mMaple

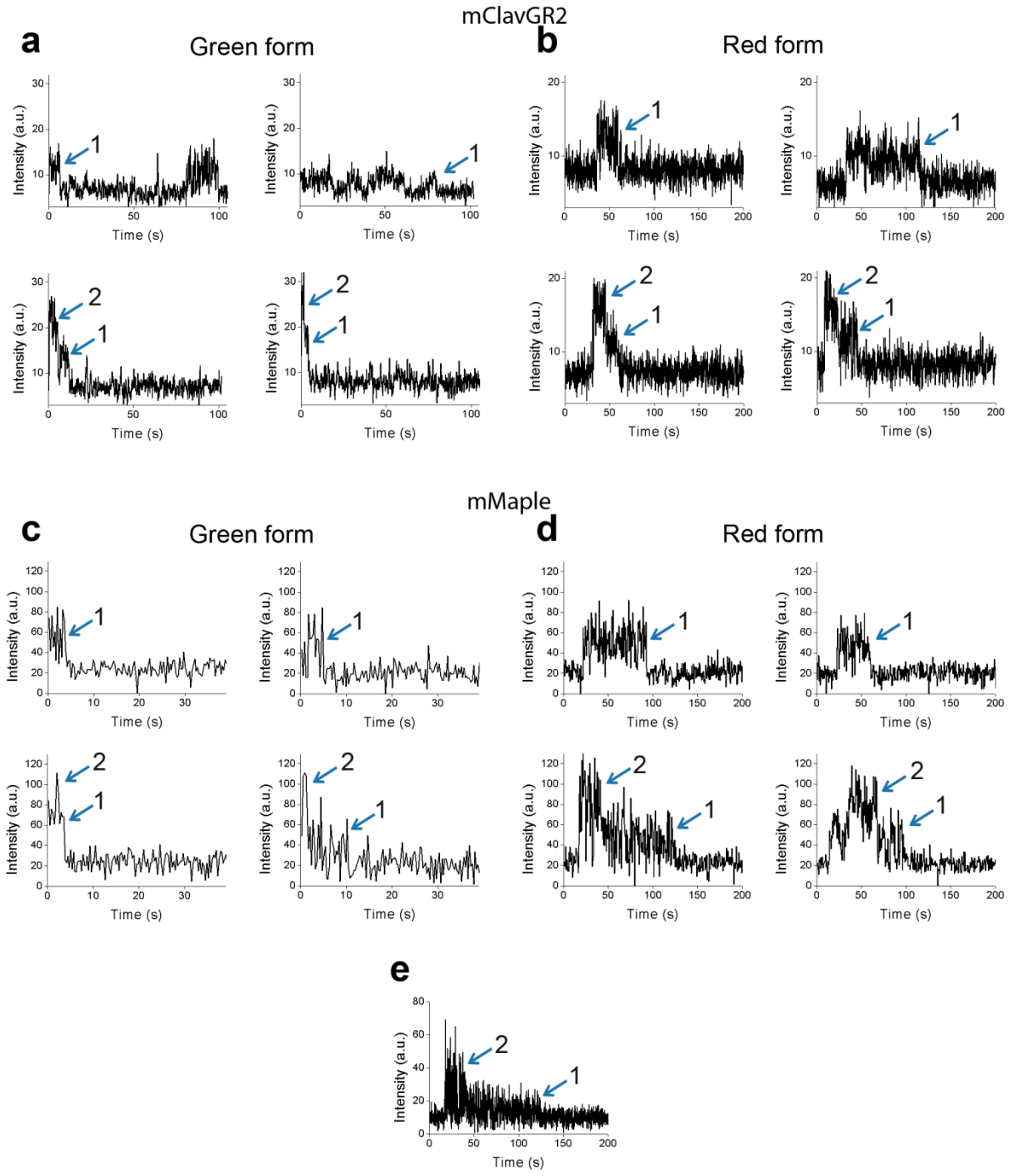

(a) Example intensity-time traces that show single (upper) and double (lower) steps obtained from the native (green) form of mClavGR2. (b) Example intensity-time traces that show single (upper) and double (lower) steps obtained from the red form of mClavGR2 after photoconversion with 405 nm laser illumination. All traces have been averaged using a rolling average of adjacent two points in the trace to smooth noise. (c) Example intensity-time traces that show single (upper) and double (lower) steps obtained from the native (green) form of mMaple. (d) Example intensity-time traces that show single (upper) and double

(lower) steps obtained from the red form of mMaple after photoconversion with 405 nm laser illumination. mMaple red and green forms had very intermittent fluorescence in which the fluorescent protein blinked with short off times. This behavior was unique to mMaple. To reduce the effect of this intermittent fluorescence, the traces were binned by adding the adjacent five points in the trace. The unbinned version of the first 2-step trace in (d) is shown in (e) as a comparison.

Supplementary Figure 5: Single step photobleaching with mEos3.2

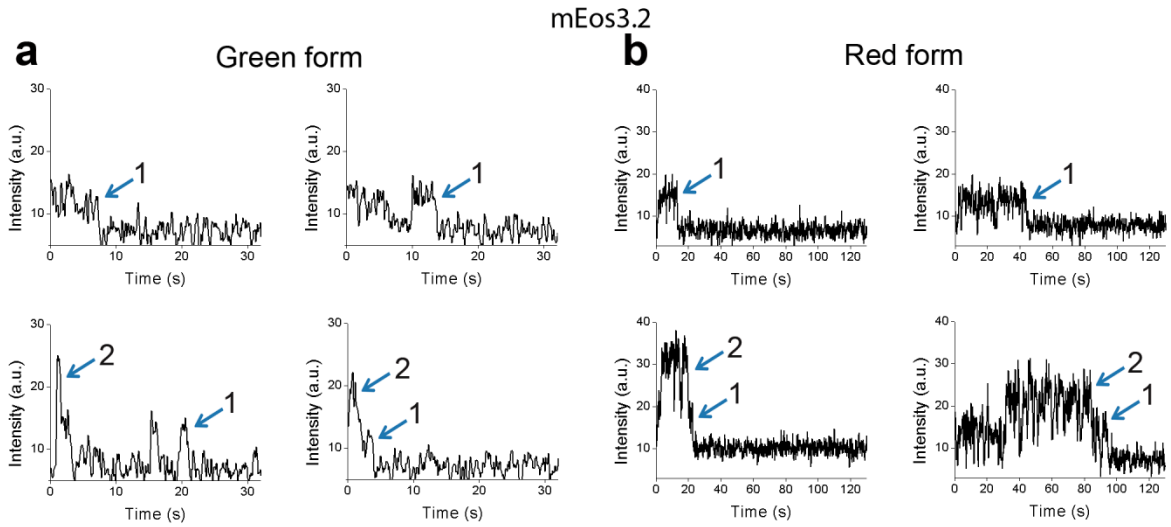

(a) Example intensity-time traces that show single (upper) and double (lower) steps obtained from the native (green) form of mEos3.2. (b) Example intensity-time traces that show single (upper) and double (lower) steps obtained from the red form of mEos3.2 after photoconversion with 405 nm laser illumination. All traces have been averaged using a rolling average of adjacent two points in the trace to smooth noise.

Supplementary Figure 6: Control experiment with untagged β- and mCherry tagged α-subunit

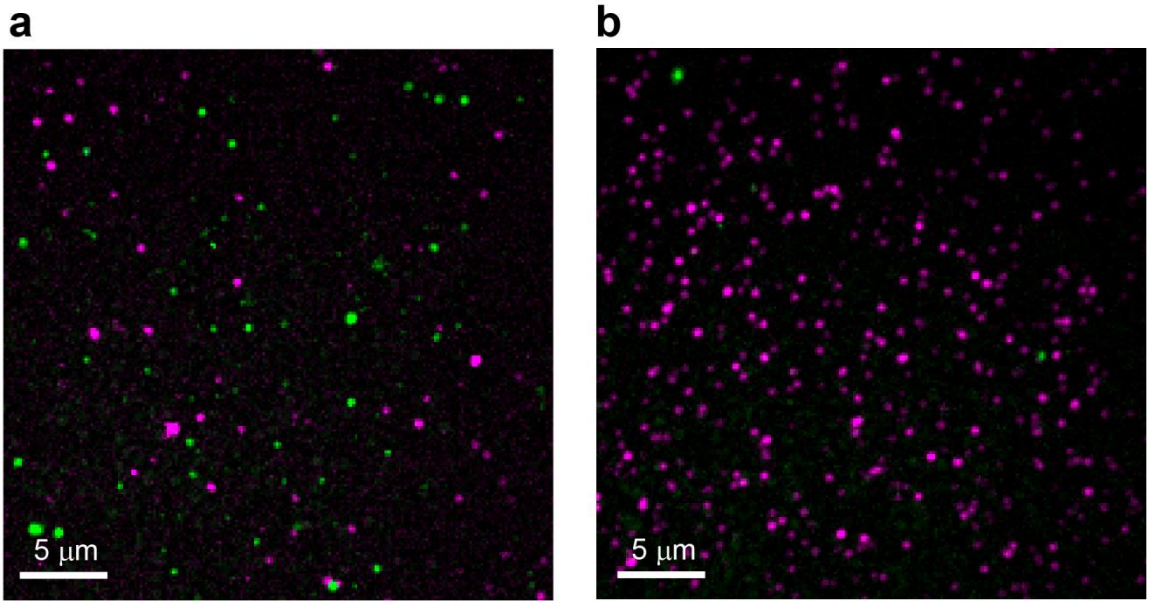

We co-expressed mCherry-tagged α-subunit together with untagged β-subunit and carried out a PALM experiment after imaging and photobleaching mCherry. Images show the overlap between mCherry-tagged α-subunit (magenta) and the maximum intensity projection of the PALM sequence for untagged β-subunit (green) immediately after fixation (a) and 1 hour after fixation (b). The spots that appear in the PALM image immediately after fixation are likely due to new GlyRs that are transported and incorporated into the cell membrane and that carry mCherry. The transport rate decreases as fixation progresses (~160 new GlyRs transported immediately after fixation, whereas 25 new GlyRs transported one hour after fixation). The coincidental overlap between the originally imaged GlyRs in mCherry (magenta) and the newly incorporated GlyRs that appear in the PALM image (green) is very low (on average <<4% determined at different time points after fixation).

Supplementary Figure 7: Single molecule counting-PALM with mEos2, mEos3.2, Dendra2, mClavGR2 and mMaple

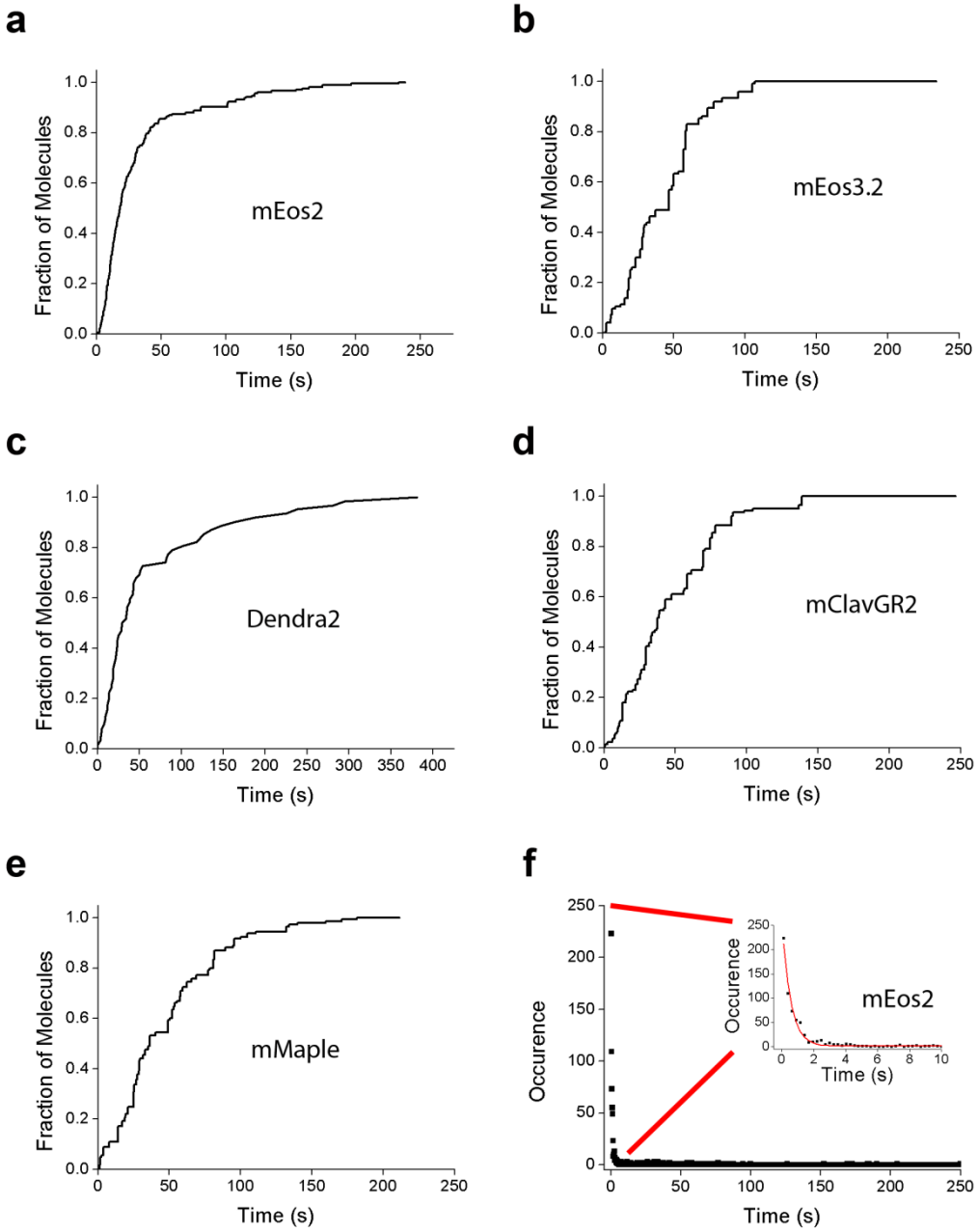

Cumulative number of counted mEos2 (a), mEos3.2 (b), Dendra 2 (c), mClavGR2 (d) and mMaple (e) molecules during PALM imaging sequence. The cumulative plots have been normalized by the maximum counted number of molecules. They show an initial rise reaching a plateau towards the end of the imaging period, indicating that the majority of the fluorescent proteins have been exhaustively imaged. (f) Distribution of fluorescence off-times in PALM traces of mEos2 tagged β-subunit (black squares: experimental data, red line: fit to an exponential decay). The time for which the exponential decayed down to 99.8% of its initial value was taken as a cut-off time (4.1 seconds) and peaks that appeared in intervals shorter than this cut-off time were linked together as belonging to the same fluorescent protein.

Supplementary Figure 8: Super-resolution localization of channels

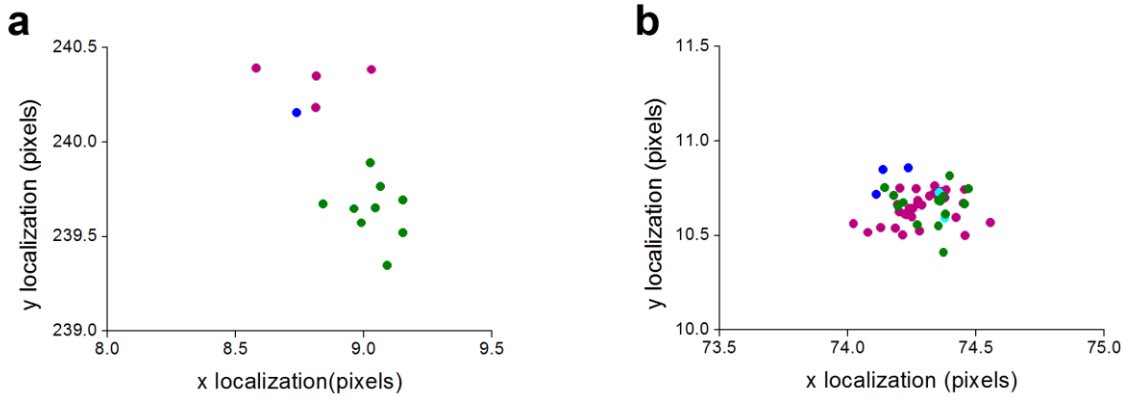

To determine the exact origin of traces that contained more than 2 peaks, we considered the precise x- and y-positions of each peak within a trace. We determined the precise x- and y-positions similar to previous methods by using custom written Python software. Briefly, a 5 X 5 pixel region centered around the maximum intensity pixel was fit to a normalized 2-dimensional Gaussian function to determine the centroid position. We color-coded each localization according to the time in which they appeared in the PALM sequence, with localizations that appeared in a time shorter than the cut-off time coded with the same color. We reasoned that, due to the intrinsic super-resolution ability, overlapping GlyRs will appear as separate clusters of localizations. The plots above show typical examples of localization data for mEos2. Indeed, a small percentage of GlyRs (4%) showed two nearby spatiotemporal clusters of localizations, whose center of mass was separated by 100 nm or more (a), whereas the localizations in the remainder of GlyRs overlapped (b). The multi-peaks in this remaining percentage are likely due to the re-activation of the same fluorescent protein after a long dark time. Consistent with this interpretation, monomeric calcium channel tagged with mEos2 leads to 4% double steps in single step photobleaching experiments but a higher percentage of double peaks (15%) in single molecule counting-PALM experiments (see Supplementary Table 1).

It is possible to correct the single molecule counting-PALM results for the overlapping GlyRs and reactivation events. In the case of overlapping GlyRs, each cluster can be re-assigned to the correct category. For example the two clusters in (a) can be reassigned as single (green) and double (magenta and blue). After this correction for mEos2, n_{single} = 89 traces contain single, n_{double} = 81 traces contain double and n_{multi} = 15 traces contain more than two peaks. To correct for reactivation, we assume that all the traces containing more than two peaks belong to the double-peak category. Thus, this category can further be corrected by adding the n_{multi} = 15 traces (n_{double} = 81+15=96). A final correction is needed for the single peaks that reactivated and were falsely assigned to the double-peak category. Assuming ~10% reactivation efficiency, the single peaks will be underestimated by ~10%. Therefore, the single peaks should be corrected from n_{single} = 89 to n_{single} = 99 (10% correction) and the corresponding number must be subtracted from the double-peak category, bringing it down to n_{double} = 86. After these corrections, the photoactivation efficiency is unchanged. Similar

results were obtained for other fluorescent proteins. Therefore, the overlapping GlyRs and the reactivation events have little, if any, impact on the calculated photoactivation efficiency.

Supplementary Figure 9: Single step photobleaching with PA-GFP and PA-mCherry

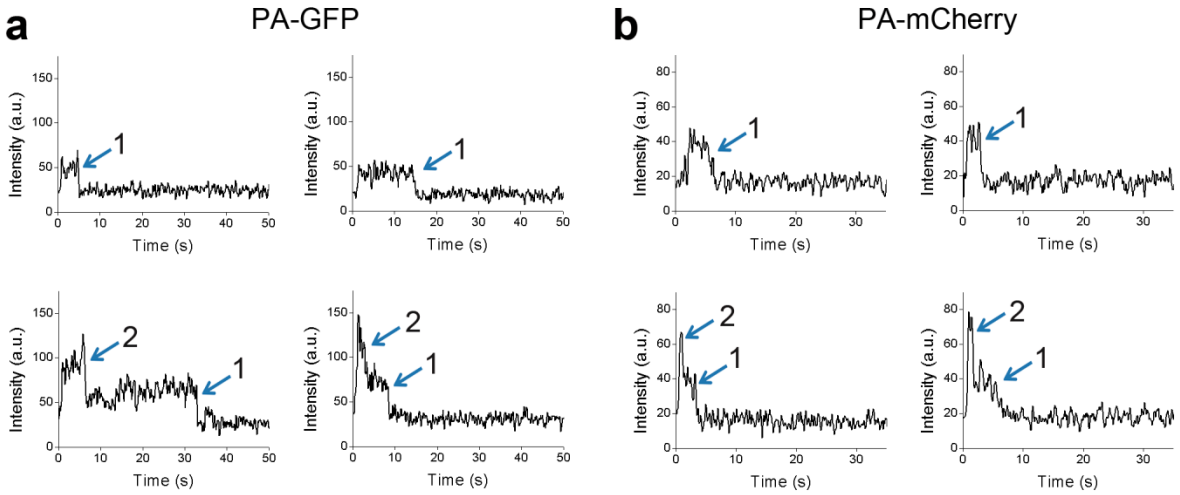

Example intensity-time traces that show single (upper) and double (lower) steps obtained from PA-GFP (a) and PA-mCherry (b) after photoactivation with 405 nm laser illumination. All traces have been averaged using a rolling average of adjacent two points in the trace to smooth noise.

Supplementary Figure 10: Fit of α1E-Ca^{+2}, β- and α-subunit data to different binomial models

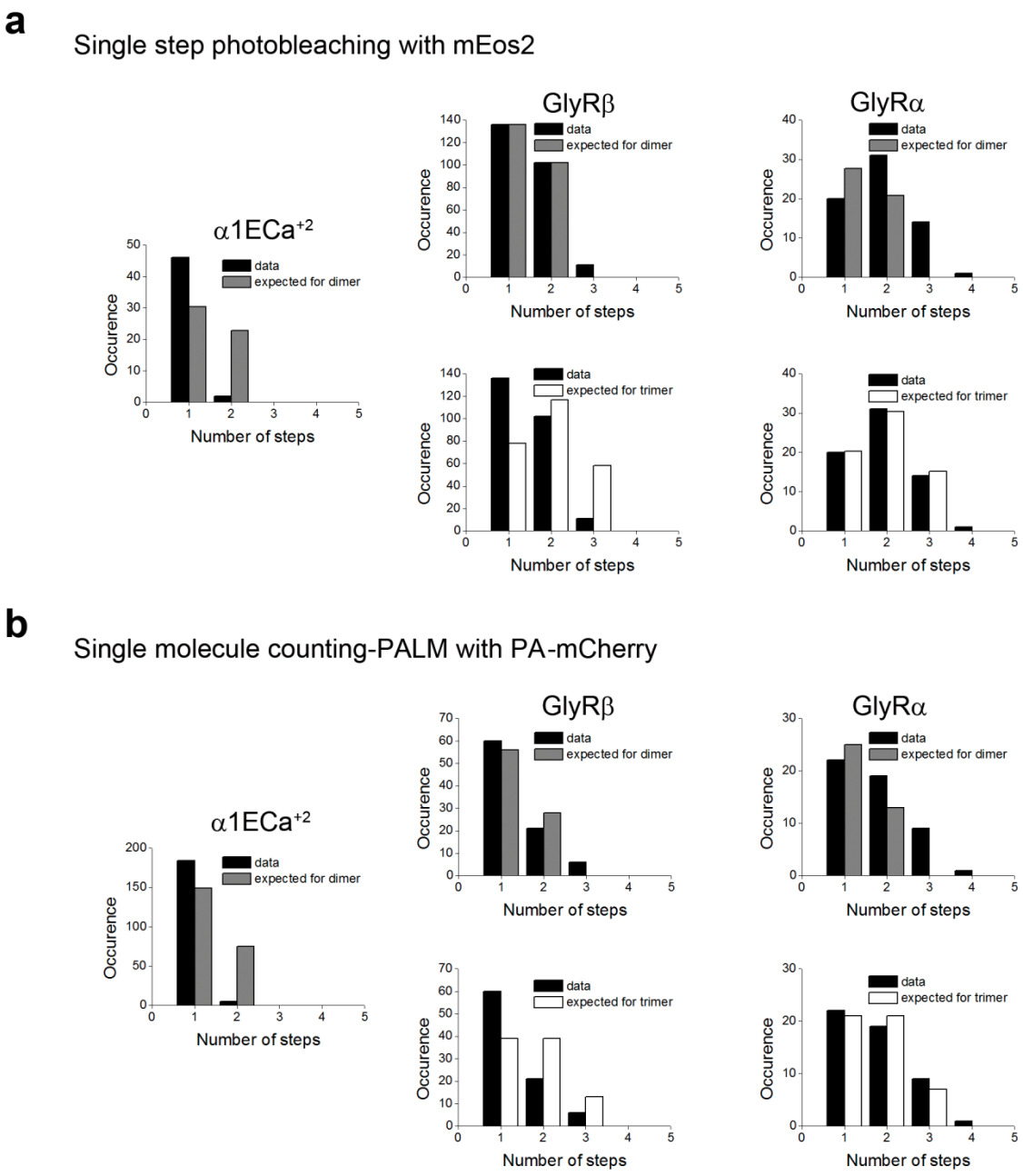

To determine if it is possible to distinguish between monomeric, dimeric and trimeric stoichiometry using these fluorescent proteins and binomial statistics either with single step photobleaching or with single molecule counting-PALM, we fit the observed data to different binomial models. For the single step photobleaching with mEos2 (a) and single molecule counting-PALM with PA-mCherry (b), the distributions of counted steps (black bars) in the case of α1E-Ca^{+2} (left), β-subunit (middle) and α-subunit (right) of GlyR are plotted. We also included here traces that showed extra steps (or peaks) than what was expected for that stoichometry. In addition, the distributions of expected steps for a dimeric (grey bars) and trimeric (white bars) stoichiometry are shown. The expected distributions were calculated by

fixing the photoactivation efficiency to 60% for mEos2 and 50% for PA-mCherry in all cases. In the case of α1E-Ca^{+2}-mEos2 and α1E-Ca^{+2}-PA-mCherry, the expected distributions for the dimeric stoichiometry deviated considerably from the observed distributions (the residual calculated as $\sqrt{\sum_i (Observed_i - Expected_i)^2}$ was 26.98 for α1E-Ca^{+2}-mEos2 and 77.82 for α1E-Ca^{+2}-PA-mCherry). In the case of β-mEos2 and β-PA-mCherry, the expected distributions that fit best to the observed data were the distributions for the dimer (residuals for β-mEos2 were 11.0 for dimer versus 76.45 for trimer and residuals for β-PA-mCherry were 10.04 for dimer versus 28.53 for trimer). In the case of α-mEos2 and α-PA-mCherry, the expected distributions that fit best to the observed data were the distributions for the trimer (residuals for α-mEos2 were 19.0 for dimer versus 1.69 for trimer and residuals for α-PA-mCherry were 11.54 for dimer versus 3.15 for trimer).

Supplementary Figure 11: Photon distribution for mEos2 and Dendra2

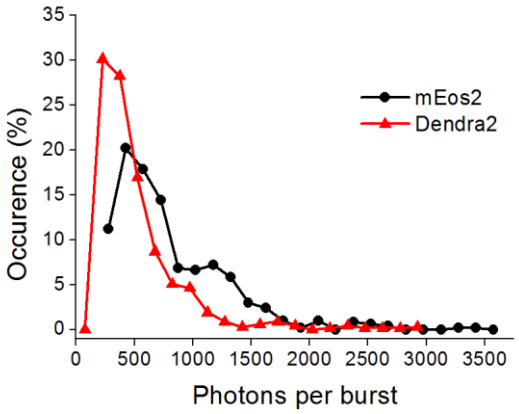

We calculated the photon distribution similar to previous methods. Briefly, a 5 X 5 pixel region centered around the maximum intensity pixel was fit to a normalized 2-dimensional Gaussian function (which included an offset parameter to correct for background signal). The area under the curve was determined and converted to the number of photons by taking into account the conversion factor appropriate for the EMCCD gain used. Shown is the photon distribution per burst for mEos2 and Dendra2 after applying a similar threshold to the one we used in selecting peaks from the PALM traces. The distributions obtained match well with previous literature[1].

Supplementary Figure 12: Simulations of stepwise photobleaching traces

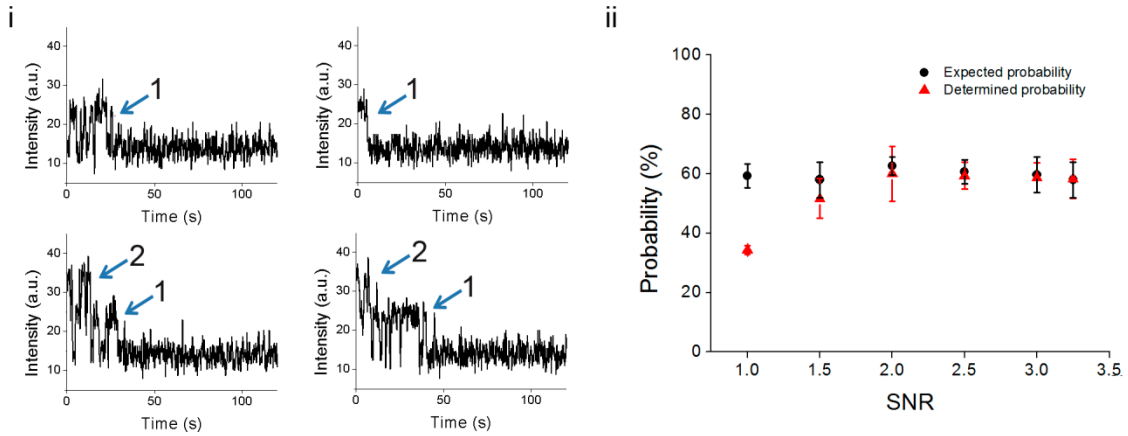

(a) We generated computer simulated traces (see Methods and (i) for examples of simulated single and double step traces) using simulation parameters with P_f = 60%, τ_{bleach} = 100 s, τ_{blink} = 2 s and signal to noise ratio (SNR, defined as the average signal divided by the standard deviation of the signal) of 3. These parameters were used to reproduce the experimental values obtained for mEos2. We then manually counted three sets of 100 simulated traces and obtained a very similar probability to the one that was expected. In addition, we determined the effect of SNR on the accuracy of manual counting by once again counting three sets of 100 simulated traces and gradually decreasing the SNR. We found that the manual counting results (ii, red) produced the expected probability (ii, black) as long as the SNR was 1.5 or higher. The uncertainties in the plot are calculated as the standard deviation of the three sets of measurements. We calculated the SNR for the photoactivated or photoconverted form of the various fluorescent proteins to be 3.18±0.51 for mEos2, 3.03±0.57 for mEos3.2, 2.77+/-0.73 for Dendra2, 1.96±0.31 for mClavGR2, 2.28±0.36 for mMaple, 2.68±0.61 for PA-mCherry and 2.33±0.28 for PA-GFP.

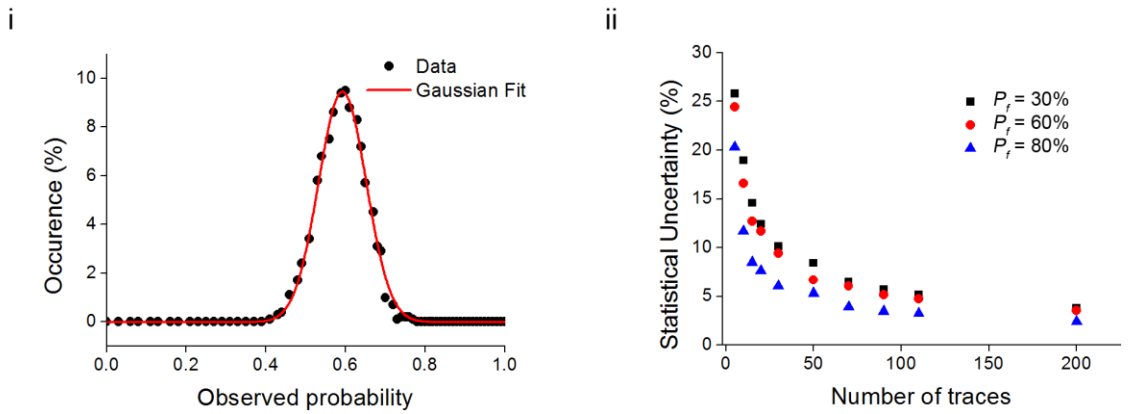

(b) For determining how the statistical uncertainty depends on the number of traces considered (*N*), we simulated *N* traces 1000 times using the same simulation parameters as above. For each of the 1000 simulations we calculated the probability for the fluorescent

protein to be "on" by considering the number of steps obtained from that particular simulation. We generated a histogram of all the observed probabilities from the 1000 simulations and fit the histogram to a Gaussian distribution (i) to determine the statistical uncertainty (the sigma parameter from the fit). For example, consider an experiment that had two photobleaching outcomes (single step and double step) and that contained $N = 70$ traces. There would be 71 different combinations of photobleaching outcomes and by simulating 70 traces we generated one of these possible combinations. One such combination would be to observe 49 traces with 1 photobleaching step and 21 with 2 photobleaching steps giving a probability of 0.46 for the fluorescent protein to be "on". This procedure was then repeated 1000 times to generate a histogram of all the observed probabilities and to calculate the uncertainty for $N = 70$ traces. Finally, the simulation was repeated by varying the number of traces (from $N = 5$ to $N = 200$) and the statistical uncertainty for each N was plotted (ii). As expected, for the three probabilities considered for the fluorescent protein to be "on" (P_f = 30%, P_f = 60% and P_f = 80%), for small N ($N < 50$) the statistical uncertainty was large but this uncertainty went down to $\leq$5% for $N = 100$ and higher (ii). Therefore, scoring 100 or more traces from experimental data should allow us to determine the fluorescent protein photoactivation efficiency with small uncertainty.

Supplementary Table 1: Number of single and double steps obtained from the fluorescent protein tagged α1E-Ca^{+2} channel

	Single step photobleaching			Single molecule counting PALM		
Fluorescent Protein	**Number of traces with 1-step**	**Number of traces with 2-steps**	**% traces with 2-steps**	**Number of traces with 1-peak**	**Number of traces with > 1 peaks**	**% traces with > 1 peaks**
mEos2	46	2	4%	101	18	15%
PA-mCherry	25	1	4%	184	6	3%

Supplementary Table 2: Primers used for PCR amplification of fluorescent proteins

Fluorescent Protein	Primers	Sequence (5´-3´)
mEos2	mEos Left 5(Kpn)	ATCCACCGGTCGGTACCAATGAGTGCGATTAAGCC
	mEos Right 3(Kpn)	ATCTAGAGTCGCGGCCGGGTACCAGTCTGGCATTGTC
mEos3.1	mEos Left 5(Kpn)	ATCCACCGGTCGGTACCAATGAGTGCGATTAAGCC
	mEos Right 3(Kpn)	ATCTAGAGTCGCGGCCGGGTACCAGTCTGGCATTGTC
mEos3.2	mEos Left 5(Kpn)	ATCCACCGGTCGGTACCAATGAGTGCGATTAAGCC
	mEos Right 3(Kpn)	ATCTAGAGTCGCGGCCGGGTACCAGTCTGGCATTGTC
mClavGR2	5mClavGR2.KpnI	ACTTTAAGAAGGAGATATAGGTACCCATGGTGAGCAAGGGCGAGGAGACC
	3mClavGR2.KpnI	ATCAAGCGAGCTCCGGTACCTTGTACAGCTCGTCCATGCCGGGC
mMaple	5 mMaple Kpn	TAAGAAGGAGATATAGGTACCCATGGTGAGCAAGGGCGAGGAGACC
	3 mMaple Kpn	ATCAAGCTAGCTCCGGTACCTTGTACAGCTCGTCCATGC
Dendra2	5Dendra2Kpn	ACTTTAAGAAGGAGATATAGGTACCCATGGAAACCCCGGGAATTAACCTG
	3Dendra2Kpn	TCAAGCGAGCTCCTGGTACCAGCACCTGGCTGGGCAGGGGGC
PA-GFP	5 PAGFP Kpn	CGAGGATCCACCGGTCGGTACCAATGGTGAGCAAGGGCGAGGAGC
	3 PAGFP Kpn	TCTAGAGTCACGGCCGCGGTACCATGTACAGCTCGTCCATGCC
PA-mCherry	5 PAmCherry Kpn	AGATCAGCTAGCGGTCGGTACCAATGGTGAGCAAGGGCGAGGAGG
	3 PAmCherry Kpn	TGAGCTCGAGATCTGAGTGGTACCTTGTACAGCTCGTCCATGCCGCC
mEos2	5mEos SpeI	ATAATAATAATAATAACTAGTGGTGGCAGCGGAGGCAGCCGCGGATCTGGAGGT AGTGGCGGAATGAGTGCGATTAAGCCAGACATGAAGATC
	3mEos. SpeI	TGGTATGGCTGATTATGAACTAGTGTCGCGGCCGCTTATCGTCTGG
PA-mCherry	5PamChy. SpeI	ATAATAATAATAATAACTAGTGGTGGCAGCGGAGGCAGCCGCGGATCTGGAGGT AGTGGCGGAATGGTGAGCAAGGGCGAGGAGGATAACATG
	3PamChy. SpeI	TGGTATGGCTGATTATGAACTAGTGTCGCGGCCGCTTACTTGTACAGCTC

Supplementary Note 1: Generality of the single step photobleaching and single molecule counting-PALM methods for determining fluorescent protein photoactivation efficiency

Here, we take advantage of the well-defined stoichiometry of the GlyR and the well-controlled expression levels in *Xenopus* oocytes to provide a comprehensive characterization of the photoactivation efficiency of eight photoconvertible and photoactivatable fluorescent proteins. However, the results presented here are not limited to the GlyR expressed in oocytes and in the future if super-resolution users need to characterize newly developed fluorescent proteins they can take advantage of any protein complex with a well-defined stoichiometry as well as tandem repeats of fluorescent proteins fused to a protein of interest and expressed in the model system of their choice. Single step photobleaching or single molecule counting-PALM combined with binomial statistics can be applied to such systems as long as care is taken to have a low enough expression level such that each "unit" can easily be spatially resolved (either at conventional fluorescence level or with super-resolution), is stationary and can be characterized individually such that statistics can be properly built. It is important to note that mobile proteins and proteins that cluster into a heterogeneous population of oligomers are not suitable nanotemplates for this type of characterization.

Supplementary Note 2: Effect of polarization on the percentage of detected fluorescent protein in PALM

While our lasers are linearly polarized, we do not believe that laser polarization and molecular orientation effects play a major role in undetected molecules for the following reasons:

1. The fluorescent proteins are inserted into the long intracellular loop between transmembrane domains TM3 and TM4[2] with a flexible linker. This intracellular loop should allow sufficient degree of mobility. Single step photobleaching results we report in the manuscript are mainly from living cells in which the fluorescent proteins likely have rotational freedom.

2. In single step photobleaching experiments, we measure 80% - 90% photoactivity of green mEos2, green Dendra2 and PA-GFP, whereas in these same experiments we measure 40% - 60% photoactivity of red mEos2, mEos3.2, Dendra2, mClavGR2, mMaple and PA-mCherry. It is highly unlikely that the 40% - 60% photoactivity we measure in single step photobleaching is due to molecular orientation and laser polarization effects. These should affect the different fluorescent proteins similarly.

3. The photoactivation efficiency determined from single step photobleaching of mEos2 is the same in living (60 ± 2%) and fixed cells (57 ± 2%), indicating that the fixation does not lead to immobilization of the fluorescent protein.

4. The step sizes of individual photobleaching steps for mEos2 are similar in living and fixed cells as shown below. In living cells the average step size is 21 ± 7 counts and in fixed cell it is 20 ± 7 counts. In addition, the photon distribution determined from single molecule counting-PALM experiments shows consistent results to previous literature (see **Supplementary Fig. 11**).

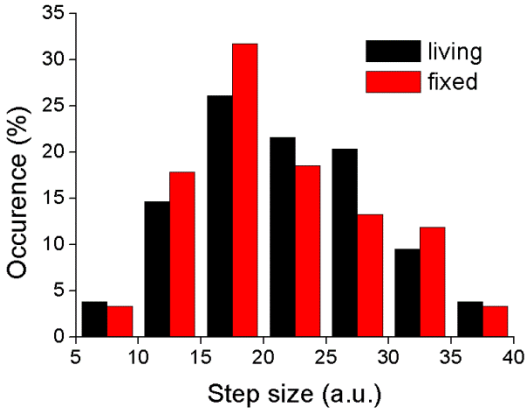

5. Both single step photobleaching and single molecule counting-PALM gives similar photoactivation efficiency for mEos2 when a quarter wave plate is used to convert the polarization of the exciting and activating light to circular polarization (see text).

However, it is important to note that in experiments where the fluorescent protein lacks rotational freedom, polarization effects may become more pronounced, leading to additional missed molecules.

Supplementary Note 3: Effect of background and threshold on the percentage of detected fluorescent protein in PALM

It is important to emphasize that the photoactivation efficiency we determine here may further be affected by high background and/or setting the threshold for identified molecules too high. In our experiments, since we are using TIRF illumination, the background is low and relatively uniform, changing by about 20-25% across the entire field of view (i.e. the background is 20-25% lower at the edge of the field of view compared to the center due to the TIRF illumination pattern). Figure below shows how the background fluorescence due to the oocyte membrane varies across the field of view in a PALM experiment.

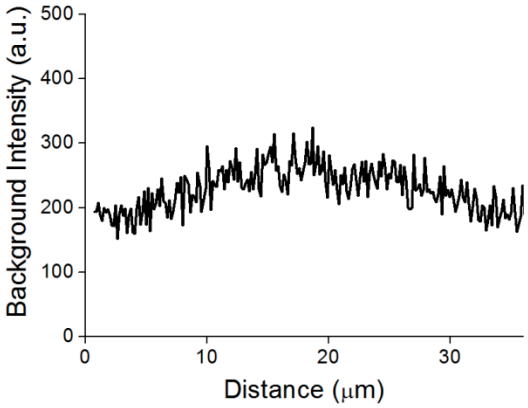

However, in experiments where proteins on intracellular structures are imaged instead of a membrane protein, highly inclined illumination is used in place of TIRF illumination to allow excitation deeper inside the cell. In such cases the background fluorescence may become higher and non-uniform due to out-of-focus fluorescence. As a result, in regions that contain high background fluorescence, additional molecules may be lost.

Similarly, it is important to set the detection threshold properly in order to not over- or undercount molecules. We find that for mEos2, the number of detected "molecules" goes down as the threshold is increased up to a certain threshold value (see below). Further increasing the threshold does not lead to a major change in the number of detected molecules for a range of thresholds. After this range, further increasing the threshold once again leads to a decrease in the number of detected molecules. In the range where the detected number of molecules is mostly constant, the photoactivation efficiency calculated for mEos2 varies between 60% and 63%. In addition, the percentage of traces that contain more than 2 peaks is also constant at around 11%. For the very low thresholds, the percentage of traces that contain more than 2 peaks is very high (~40%) indicating detection of a large number of false positives. Similar behavior is obtained for the other fluorescent proteins. In single molecule counting-PALM experiments, a similar characterization can be done (plotting the number of detected molecules versus threshold used) to guide the choice of threshold.

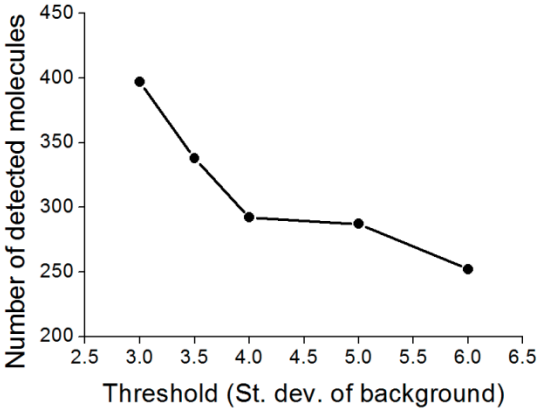
Number of detected molecules
450
400
350
300
250
200
2.5
3.0
3.5
4.0
4.5
5.0
5.5
6.0
6.5
Threshold (St. dev. of background)

Supplementary References

1. Lee, S.H., Shin, J.Y., Lee, A. & Bustamante, C. Counting single photoactivatable fluorescent molecules by photoactivated localization microscopy (PALM). *Proc Natl Acad Sci U S A* **109**, 17436-17441 (2012).
2. Rajendra, S., Lynch, J.W. & Schofield, P.R. The glycine receptor. *Pharmacol Ther* **73**, 121-146 (1997).